INFECTION AND IMMUNITY, July 2006, p. 3783–3789 Vol. 74, No. 7
0019-9567/06/$08.00+0 doi:10.1128/IAI.00022-06

Cell Wall-Mediated Neuronal Damage in Early Sepsis

Carlos J. Orihuela,[1]†‡ Sophie Fillon,[1]† S. Hope Smith-Sielicki,[1] Karim C. El Kasmi,[1] Geli Gao,[1] Konstantinos Soulis,[1]§ Avinash Patil,[2] Peter J. Murray,[1] and Elaine I. Tuomanen[1]*

Department of Infectious Diseases, St. Jude Children's Research Hospital, 332 N. Lauderdale Rd., Memphis, Tennessee 38105,[1] and University of Tennessee Medical School, Dunlap Ave., Memphis, Tennessee 38163[2]

Received 4 January 2006/Returned for modification 27 March 2006/Accepted 20 April 2006

Neuronal dysfunction can occur in the course of sepsis without meningitis. Sepsis-associated neuronal damage (SAND) was observed in the hippocampus within hours in experimental pneumococcal bacteremia. Intravascular challenge with purified bacterial cell wall recapitulated SAND. SAND persisted in PAFr$^{-/-}$ mice but was partially mitigated in mice lacking cell wall recognition proteins TLR2 and Nod2 and in mice overexpressing interleukin-10 (IL-10) in macrophages. Thus, cell wall drives SAND through IL-10-repressible inflammatory events. Treatment with CDP-choline ameliorated SAND, suggesting that it may be an effective adjunctive therapy to increase survival and reduce organ damage in sepsis.

During sepsis, organ dysfunction occurs independently of invasion of the organ by circulating bacteria. In the case of early encephalopathy, which occurs in up to 70% of septic patients in intensive care units (42), the pathogenesis is unclear, as it precedes peripheral organ dysfunction and bacterial invasion of the central nervous system (CNS). It is assumed that intravascular inflammation deleteriously affects neuronal function at a distance (i.e., across the blood-brain barrier) since the vascular compartment and the CNS communicate bidirectionally during infection (38). For example, production of the late mediator of sepsis HMGB1 is inhibited by acetylcholine released from the vagus nerve in response to systemic lipopolysaccharide (LPS) (51). Conversely, intraperitoneal lipopolysaccharide induces intracerebral expression of TLR2 (21), interleukin-6 (IL-6) (50), and IL-1β (49); activates microglia in the dentate gyrus; decreases hippocampal neurogenesis (29); and causes alteration of neuronal function (18). Greater understanding of how these effects are related to neurological damage is required for the design of therapeutic interventions.

Streptococcus pneumoniae is a gram-positive bacterium reported to have the highest case fatality rate (14.5%) of all organisms causing pediatric sepsis (52). Patients are noted for devastating neurological sequelae even in the absence of meningitis (39). However, the mechanism of neuronal injury has been studied only in the context of meningitis, where the presence of a threshold of $>10^5$ pneumococci/ml in the subarachnoid space induces strong inflammation, a response that is recapitulated by purified pneumococcal cell wall (47, 48). Neuronal damage during meningitis arises from a combination of direct cytotoxicity of bacterial components and activation of the host response (3, 19, 20, 25, 35). Apoptosis of neurons in the dentate gyrus of the hippocampus is particularly prominent both in animal models (3–5, 43) and at human autopsy (31), and detailed analysis has indicated that it arises by both caspase-dependent and -independent pathways. However, the effect of pneumococcal bacteremia on neurons remains unknown. While studying the development of meningitis during sepsis in mice, we observed that neuronal damage was evident prior to entry of bacteria into the subarachnoid space. Although the precise neuropathology associated with septic encephalitis in humans is unknown, the occurrence of CNS injury in an animal model of sepsis could be informative as to possible mechanisms. We sought to dissect the pathogenesis of sepsis-associated neuronal damage (SAND) and distinguish its underlying mechanism from other pathological effects of bacterial components.

MATERIALS AND METHODS

Bacterial strains and components. *S. pneumoniae* serotype 4, strain TIGR4 (44), or unencapsulated strain R6 was grown on tryptic soy agar (Difco, Detroit, MI) plates supplemented with 3% defibrinated sheep blood or in defined semisynthetic casein liquid medium supplemented with 0.5% yeast extract (45). Mutants of TIGR4 lacking pneumolysin (*ply*), pyruvate oxidase (*spxB*), or both were created by insertion-duplication mutagenesis as previously described (40, 56). Erythromycin (1 μg/ml; Sigma) was added to the growth medium of the mutants as appropriate.

Highly purified cell wall was prepared from R6 as described previously (47). Bacteria were boiled in sodium dodecyl sulfate; mechanically broken by being shaken with acid-washed glass beads; and treated sequentially with DNase, RNase, trypsin, LiCl, EDTA, and acetone. Peptidoglycan free of teichoic acid was prepared from insoluble cell wall by treatment with 48% hydrofluoric acid (15). High-pressure liquid chromatography and mass spectrometry confirmed the purity and identity of the cell wall preparations. The absence of contaminating endotoxin in the purified cell wall sample was confirmed by the *Limulus* test (Associates of Cape Cod Inc.).

Model of SAND. All experimental procedures were done with 4- to 5-week-old mice unless otherwise indicated, and wild-type littermates (BALB/c, C57BL/6, or FVB) were tested in parallel as controls. Wild-type mice of different genetic backgrounds experienced the same degree of SAND. The following mice were maintained in biosafety level 2 facilities at the St. Jude Children's Research Hospital Animal Facility: female BALB/c mice (Jackson Laboratory), IL-10$^{-/-}$ mice (Jackson Laboratory), IL-10-transgenic mice overexpressing IL-10 in macrophages (23), TLR2$^{-/-}$ mice (Jackson Laboratory), C57BL/6 wild-type mice and Nod2$^{-/-}$ mice (33), tumor necrosis factor (TNF) receptor 1- or 2-deficient mice (TNFrsf1a^{tm1Mak} [34] and TNFrsf1b^{tm1Mwm} [10] mice), caspase 3$^{-/-}$ mice

* Corresponding author. Mailing address: Infectious Diseases, St. Jude Children's Research Hospital, Mailstop 320 IRC 8057, 332 N. Lauderdale Rd., Memphis, TN 38105. Phone: (901) 495-3114. Fax: (901) 495-3099. E-mail: elaine.tuomanen@stjude.org.

† These authors contributed equally to this work.

‡ Present address: Department of Microbiology and Immunology, University of Texas Health Science Center at San Antonio, 7703 Floyd Curl Drive, MC7758, San Antonio, TX 78229-3900.

§ Present address: Papaflessa 152, 185 46 Peiraias, Greece.

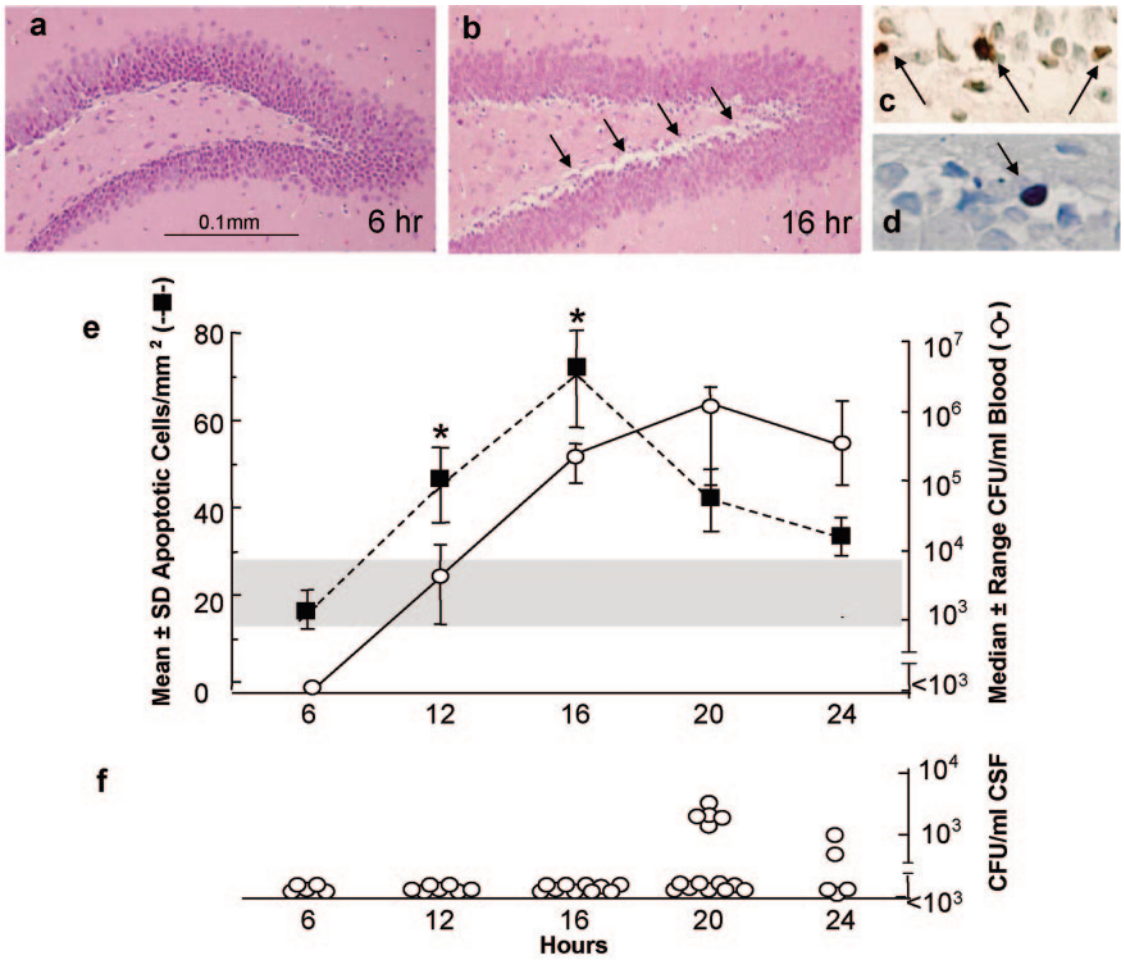

FIG. 1. Relative time course of SAND and bacteremia. BALB/cJ mice were challenged intranasally with 10^7 CFU of pneumococci (n = 5, 7, 10, 14, and 5 animals at 6, 12, 16, 20, and 24 h, respectively). (a and b) Representative H&E histopathology of dentate gyrus is shown for no damage (a) (6 h) and peak damage (b) (16 h; arrows indicate area of damage; magnification, ×7.5; marker, 0.1 mm). (c) Representative TUNEL-positive neurons (arrows; magnification, ×33.75). (d) Representative neuron stained for cleaved caspase 3 (arrow). (e) Mean number ± standard deviation of apoptotic cells/mm^2 in the dentate gyrus over time (squares) was correlated with bacterial titers (circles) in the blood (median ± range, 5th and 95th percentiles; lower limit of detection, 10^3 CFU/ml). The shaded region indicates the range of apoptosis/mm^2 in PBS control animals (n = 2/time point). The asterisks indicate significant differences from PBS at P = 0.014 and P = 0.017. (f) Individual CSF bacterial titers over time.

(26), PAFr$^{-/-}$ mice (36), and N-tg (*Gfap-luc*)-Xen mice to track astrocyte activation by injury (Xenogen, Alameda, CA) (9). Per group, 5 to 10 mice received T4 bacteria intranasally (1×10^7 CFU per 25 μl) or 5×10^7 bacterial equivalent CFU of heat-killed R6 bacteria or 10^6 or 10^7 bacterial equivalents of purified cell wall in 100 μl phosphate-buffered saline (PBS) intravenously. Bioluminescence was measured using the Xenogen IVIS camera at 24, 48, 72, and 96 h, 10 min after injection of the substrate luciferin (Xenogen; 150 mg/kg of body weight intraperitoneally). In order to detect the basal expression of glial fibrillary acidic protein (GFAP), GFAP-Luc mice were also injected with PBS as a negative control and littermate GFAP-negative mice did not show any basal bioluminescence after injection of luciferin. In a subset of experiments, mean arterial blood pressure was measured with a catheter placed in the femoral artery (17) and blood was sampled for pH at time zero and 24 h. Blood pressure as well as blood pH was within physiological range, and no difference over time or between controls and infected animals was detected (data not shown). For some experiments, mice received 10 μg/g of a neutralizing polyclonal goat anti-mouse TNF alpha (TNF-α) immunoglobulin G (IgG) antibody or normal goat IgG as an isotype control (R&D Systems) intraperitoneally 1 h prior to challenge. The neutralizing activity of the anti-TNF-α antibody that was used in vivo was confirmed in an in vitro bioassay measuring cytotoxicity on L929 cells (data not shown) (11). Antibody concentrations used in the bioassay were chosen to adequately reflect concentrations used in vivo (10 μg/g in vivo, 150 μg/ml in vitro). This concentration of antibody reproducibly neutralized TNF-α cytotoxicity that was tested over a broad range (starting at 1 ng/ml, serially diluted twofold down to 0.004 ng/ml) including TNF-α levels typically detected after LPS challenge in mouse serum by enzyme-linked immunosorbent assay (ELISA) (up to 1 ng/ml). Importantly, in vitro TNF-α cytotoxicity was neutralized at even much lower concentrations (2 μg/g) of neutralizing antibody. For all experiments, a matching isotype control antibody (IgG) that did not interfere with the effect of TNF-α on cytotoxicity was used (data not shown). All experiments were done in compliance with National Institutes of Health and institutional guidelines.

For postchallenge sampling or Xenogen imaging, mice were anesthetized with either inhaled isoflurane (Baxter Healthcare) at 2.5% or MKX (1 ml of ketamine [Fort Dodge Laboratories] at 100 mg/ml, 5 ml of xylazine [Miles Laboratories] at 100 mg/ml, and 21 ml of PBS). MKX was administered by intraperitoneal injection at a dose of 0.05 ml/10 g of body weight. Mice were sacrificed at the designated time points, and cerebrospinal fluid (CSF), blood, and brain were collected for analysis. Up to 5 μl CSF was obtained by puncture of the cisterna magna, and absence of leukocytes was confirmed microscopically. CSF was plated to document bacterial number (detection limit, 10^3 bacteria/ml). Blood was collected by heart puncture and was serially diluted and plated to determine CFU/ml of blood. Mice were perfused transcardially with 3% paraformaldehyde in 0.1 mol/liter of cacodylate buffer (pH 7.4). After perfusion-fixation, the brains were removed and postfixed in 3% paraformaldehyde at 4°C overnight. The brains were then embedded in paraffin and cut into 5-μm sections. Unless indicated otherwise, all tissue samples were obtained from perfused mice.

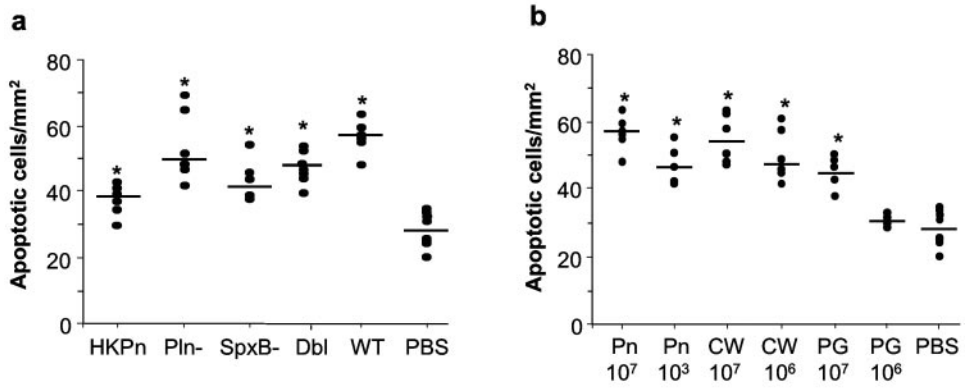

FIG. 2. Role of bacterial components in SAND. (a) Apoptosis in the dentate gyrus of C57BL/6 mice 6 h after intravenous injection of 10^7 CFU of TIGR4 bacteria (wild type [WT]; $n = 6$), an isogenic pneumolysin-deficient mutant (Pln−; $n = 6$), an isogenic pyruvate oxidase-deficient mutant unable to produce hydrogen peroxide (SpxB−; $n = 5$), double Pln/SpxB-knockout bacteria (Dbl; $n = 8$), or heat-killed bacteria (HKPn; $n = 6$) versus PBS ($n = 8$). Each mouse is an individual symbol. *, statistically different from PBS (HKPn, $P = 0.007$; Pln−, $P = 0.0003$; SpxB−, $P = 0.003$; Dbl, $P < 0.001$; wild type, $P < 0.0001$). (b) Neuronal apoptosis 6 h after intravenous injection of mice with living TIGR4 (Pn), pneumococcal cell wall (CW), or peptidoglycan (PG) at the indicated doses in CFU equivalents. *, significant difference from PBS at $P \leq 0.0007$.

Histopathology. Neuronal damage was quantitated in fixed slices of perfused brains. Neuronal damage was defined as an excess of apoptotic neurons in the dentate gyrus as determined by TUNEL (terminal deoxynucleotidyltransferase-mediated dUTP-biotin nick end labeling) staining (Serologicals, Temecula, CA) and corroborated by hematoxylin and eosin (H&E) staining versus PBS controls. H&E staining was used to assess the overall morphology, and the Scion Image program was used to measure the area of the dentate gyrus. TUNEL staining was performed on sections of brain that were adjacent to those stained with H&E (five sections/mouse). TUNEL-positive cells in the dentate gyrus were counted on slides divided into five visual fields per slide of 100 μm each, and the average number of TUNEL-positive cells was expressed as the number of apoptotic neurons/mm^2 of dentate gyrus. In all animals, the sections taken were from the middle of the brain and displayed a comparable part of the hippocampus. Cleaved caspase 3 was stained using the SignalStain Cleaved Caspase-3 IHC detection kit (Cell Signaling, Beverly, MA).

Cytokine ELISA. Blood from wild-type and PAFr$^{-/-}$ mice (10 per group) was collected at 24 h prior to and 1, 4, 8, and 12 h after injection via the tail vein with 10^7 bacterial equivalents of cell wall in 100 μl PBS or with 25 mg/kg LPS from *Escherichia coli* serotype O111:B4 (Sigma) given intraperitoneally as a positive control. Whole blood was clotted for 2 h at room temperature (RT), and serum was separated after centrifugation at 3,000 rpm for 20 min and stored at −20°C until assayed by ELISA. For the ELISA, microtiter plates (Nunc Maxisorb) were coated with the respective anti-mouse capture antibodies at 50 μl/well: IL-12 (2 μg/ml; Pharmingen), IL-10 (4 μg/ml; Pharmingen), IL-6 (2 μg/ml; Pharmingen), IL-1 (4 μg/ml; Pharmingen), gamma interferon (0.5 μg/ml; Pharmingen), and TNF-α (3 μg/ml; e-bioscience) in coating buffer (0.1 M $Na_2CO_3H_2O$, 0.1 M $NaHCO_3$) overnight at 4°C. The next day, plates were washed with ELISA washing buffer (1% Tween 20, 1 mM Tris base, 154 mM NaCl), blocked with 300 μl/well of ELISA buffer (10% fetal calf serum in PBS), and incubated for 2 h at RT. After washing, 50 μl/well of a 1/10 dilution in ELISA buffer of mouse serum and duplicate serial twofold dilutions of the respective standards (50-ng/ml starting concentration) were added and incubated overnight at 4°C. Plates were then washed three times, and biotin-conjugated detection antibodies for IL-12 (1 μg/ml; Pharmingen), IL-10 (1 μg/ml; Pharmingen), IL-6 (1 μg/ml; Pharmingen), IL-1 (300 ng/ml; Pharmingen), gamma interferon (2 μg/ml; Pharmingen), and TNF-α (1.6 μg/ml; e-bioscience) diluted in ELISA buffer were added (50 μl/well) and incubated for 45 min at RT. After the plates were washed three times, streptavidin peroxidase (Sigma) diluted 1:1,000 in ELISA buffer was incubated for 30 min at RT. Plates were soaked in washing buffer for 1 min and washed five times, the TMB peroxidase substrate system (Kirkegaard & Perry Laboratories, Maryland) was applied at 50 μl/well, reactions were stopped with 10% phosphoric acid (50 μl/well), and absorbance was measured at 405 nm in an ELISA reader (Molecular Dynamics). Cytokine concentrations were calculated according to the respective standard curves.

Dexamethasone and CDP-choline treatment. Mice were given dexamethasone (2 mg/kg; Sigma) (24, 32) or 100 μl PBS by tail vein injection. One hour later, the same mice were challenged intravenously with 10^7 CFU of TIGR4 in 100 μl PBS or only PBS. Mice were sacrificed 6 h after the second injection, the CSF was collected and examined for bacteria and white blood cells, and the animal was perfused for subsequent histopathology of brain tissue. For experiments with CDP-choline, mice were given intraperitoneal CDP-choline (500 mg/kg; Biomol) 24 h prior to being given 1×10^7 intravenous cell wall equivalents or PBS alone. Six hours after challenge, CSF was collected and examined as indicated above, and the animals were perfused for histopathology.

Statistical analysis. Student's *t* test was used unless otherwise noted.

RESULTS

Neuronal damage in the absence of meningitis. Mice were challenged intranasally with 10^7 pneumococci and followed for bacterial titers in blood and CSF for 24 h (Fig. 1e and f). Pneumococci were detectable in the bloodstream of all mice by 12 h after infection and yet were not detected in the CSF (limit of detection, 10^3 CFU/ml) until after 20 h, at which time only a minority of mice (5/14; 36%) had positive cultures. Histology failed to detect bacteria in either the ventricles or the choroid plexus, and CSF leukocytes were detected only when bacteria were present. Cells in the dentate gyrus staining positive for TUNEL (Fig. 1c) increased over time to 16 h, following which areas of neuronal loss were detected by H&E staining consistent with clearance of the nonviable cells (i.e., decrease of numbers of TUNEL-positive cells). Following intranasal challenge, SAND increased to a median of 48 cells/mm^2 at 12 h and peaked at 73 cells/mm^2 at 16 h ($P = 0.02$ versus PBS control) (Fig. 1e). Cortical neurons were not damaged and astrocyte activation was not detectable over 48 h in mice bearing the bioluminescent GFAP-Luc marker, a prominent marker of astrocyte activation during injury (9) (data not shown). Thus, the onset of neuronal damage (an excess of apoptotic neurons in the dentate gyrus as determined by TUNEL and corroborated by cellular loss by H&E staining versus PBS controls) occurred very early during bacteremia and peaked many hours prior to detection of bacteria or leukocytes in the CSF.

Damage was not secondary to decreases in either blood pH or blood pressure (data not shown). Brain sections also stained positively for cleaved caspase 3 (Fig. 1d), confirming that TUNEL-positive cells were indicative of apoptosis. Moreover,

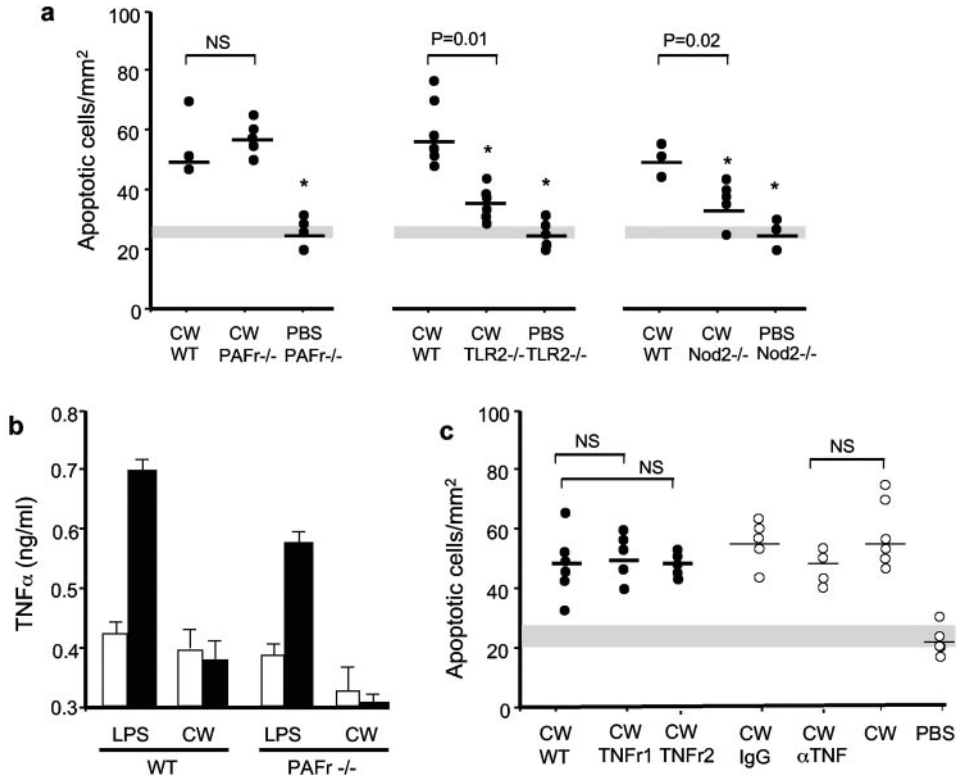

FIG. 3. SAND in wild-type and receptor-deficient mice. (a) TUNEL-positive cells/mm^2 in the dentate gyrus 6 h after intravenous injection of 10^7 CFU of cell wall (CW) in 4-week-old PAFr$^{-/-}$, TLR2$^{-/-}$, or Nod2$^{-/-}$ mice or their littermate controls (wild type [WT]). Each mouse is an individual symbol. The shaded region indicates the range of apoptosis in PBS littermate control animals. *, not significantly different from PBS in wild type at $P \leq 0.01$. (b) Mean serum TNF-α level ± standard deviation at 4 h (open bars) and 8 h (closed bars) after LPS or cell wall challenge in wild-type (wild-type littermate; $n = 10$) versus PAFr$^{-/-}$ ($n = 10$) mice. PBS-challenged animals demonstrated <0.3 ng/ml TNF-α. (c) TNFr1$^{-/-}$ or TNFr2$^{-/-}$ mice or littermate controls (filled circles) were challenged intravenously with 10^7 CFU of cell wall. Some wild-type C57BL/6 animals (open circles) received neutralizing anti-TNF-α antibody (αTNF) 1 h prior to the challenge or IgG isotype control (IgG). TUNEL-positive cells/mm^2 in the dentate gyrus were assessed at 6 h. Each mouse is an individual symbol. The shaded region indicates the range of apoptosis/mm^2 in PBS wild-type littermate control animals. NS, no significant difference from cell wall in wild-type mice.

neuronal damage was also observed in mice with low-level bacteremia (intravenous 10^3 CFU/ml). Collectively these studies suggested that modest levels of circulating pneumococci were capable of eliciting neuronal damage independently of the presence of bacteria in the CSF.

SAND caused by cell wall. Three pneumococcal components are known to induce eukaryotic cell death: the toxins pneumolysin and hydrogen peroxide and the cell wall itself (5, 12, 28). To determine which bacterial components were required for SAND, mice were infected intravenously with 10^7 living bacteria deficient in production of pneumolysin or hydrogen peroxide or both toxins or with a bolus of heat-killed bacteria. No bacteria were cultured in the CSF, but analysis of TUNEL-stained brain sections revealed that all cohorts had apoptosis in the dentate gyrus equivalent to that observed in mice infected with living, wild-type bacteria (Fig. 2a). These findings indicated that production of pneumolysin or hydrogen peroxide was not required for SAND and suggested that the responsible product was heat stable and not produced by active bacterial metabolism, features consistent with cell wall. This hypothesis was tested by injecting a bolus of 10^7 or 10^6 bacterial equivalents of purified cell wall (as determined by weight of cell wall [47]) which caused an abundance of TUNEL-positive hippocampal cells equivalent to that caused by a high dose of living bacteria (Fig. 2b). Attenuation of damage from 55 ± 8 to 42 ± 1 apoptotic cells/mm^2 ($P = 0.042$) in wild-type versus caspase 3$^{-/-}$ animals ($n = 5$), respectively, provided further evidence that cell wall-induced neuronal damage was apoptotic in nature. Damage was also noted upon challenge with 10^7 bacterial equivalents of purified peptidoglycan (macromolecular material devoid of choline teichoic acid), and peptidoglycan-induced damage was dose dependent (Fig. 2b). In contrast, 10^7 bacterial equivalents of muramyl dipeptide evoked no hippocampal apoptosis (data not shown). None of these challenge protocols resulted in damage to cortical neurons (data not shown).

Mechanism of SAND and impact of therapy. Cell walls in the peripheral circulation could potentially contribute to SAND through interactions with cell wall recognition proteins such as PAFr, TLR2, and Nod2. Neuronal damage was equivalent in wild-type and PAFr$^{-/-}$ mice, while TLR2$^{-/-}$ and Nod2$^{-/-}$ mice demonstrated significantly less neuronal damage (Fig. 3a). Examination of the cytokine response in the peripheral blood of cell wall-challenged mice demonstrated that TNF-α, IL-1β, IL-6, and other cytokine levels were very low in wild-type, PAFr$^{-/-}$, and TLR2$^{-/-}$ mice despite signif-

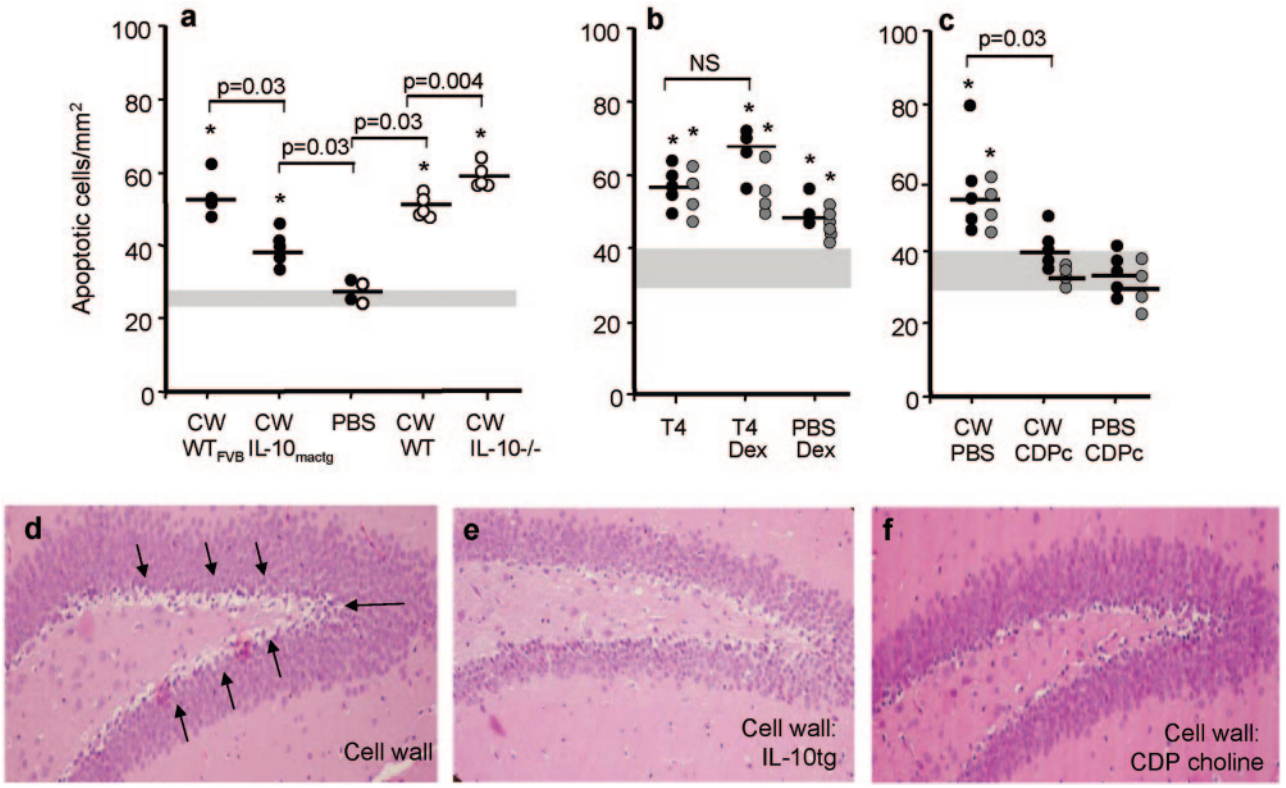

FIG. 4. Modification of SAND by anti-inflammatory interventions. Mice were challenged intravenously with 10^7 CFU pneumococci (T4) or cell wall equivalents (CW) as indicated, and neuronal apoptosis in the dentate gyrus was quantitated at 6 h compared to PBS controls (range indicated by shaded area; *, statistically different from PBS control). Each mouse is an individual symbol. (a) Filled circles, IL-10-transgenic mice (IL-10mactg) versus littermate controls; open circles, IL-$10^{-/-}$ mice versus littermate controls. (b) One-hour pretreatment of wild-type (black circles) or PAFr$^{-/-}$ (gray circles) mice with dexamethasone (Dex); NS, not statistically different. (c) CDP-choline (CDPc) administered to wild-type (black circles) or PAFr$^{-/-}$ (gray circles) mice at time of challenge. (d to f) Representative H&E histopathology for panels a and c (arrows indicate damaged area). Compare to histopathology showing no injury in Fig. 1a. WT, wild type.

icant SAND in the first two sets of mice (Fig. 3b). CSF levels of these cytokines were undetectable. Lack of correlation of SAND with elevated peripheral cytokines was consistent with high levels of SAND in TNFr1$^{-/-}$ or TNFr2$^{-/-}$ mice (Fig. 3c) and failure of neutralizing anti-TNF-α antibody to prevent SAND (Fig. 3c). Like wild-type mice, TLR2$^{-/-}$ mice (which showed less neuronal damage) showed undetectable IL-10 in the CSF or periphery.

IL-10 is a potent and broad downregulator of inflammation through many pathways including but not limited to cytokines (22). To test if such anti-inflammatory interventions could affect the level of SAND, mice overexpressing IL-10 or defective in IL-10 production were challenged with cell wall. IL-$10^{-/-}$ mice showed enhanced neuronal damage (Fig. 4a) consistent with their known excessive inflammation in response to pathogen challenge (30). Conversely, transgenic mice overexpressing IL-10 in macrophages were strongly protected against SAND (Fig. 4a and 3e).

Given the indication of damage driven by an inflammatory process but the lack of indication of a specific cytokine as a root cause, treatment with dexamethasone to broadly downmodulate inflammation was tested but failed to attenuate SAND in the PAFr$^{-/-}$ or wild-type mice (Fig. 4b). However, CDP-choline, which has been shown to ameliorate sepsis (54) and apoptosis of neurons during pneumococcal meningitis (56), strongly protected wild-type and PAFr$^{-/-}$ mice from SAND (Fig. 4d and f).

DISCUSSION

It has been known for decades that pneumococcal cell wall is a potently bioactive material and that bioactivities applicable to distinct aspects of infection can be assigned to its specific subcomponent structures (6, 41, 47, 48). For example, in the meningitis model, the capsule was poorly inflammatory while choline-bearing, insoluble cell wall was strongly inflammatory. Removal of choline teichoic acid from peptidoglycan yielded a more restricted array of bioactivities, digestion further to muramyl peptides more strongly limited inflammatory capability, and cleavage of stem peptides virtually eliminated bioactivity (6, 14, 27, 46, 48, 53). More recently, distinct molecules involved in recognition of these different cell wall subspecies have been described: TLR2 participates in the inflammatory responses of peptidoglycan while Nod2 appears to recognize the smaller, muramyl peptides (16, 55). PAFr is an important receptor mediating biological activities of choline-containing cell wall (8).

When injected into the subarachnoid space, pneumococci have been shown to induce two temporally distinct waves of apoptosis in neurons and endothelial cells (2–4, 28). While the

early wave involves toxins, the second wave at ~24 h after intracisternal challenge has been shown to involve cell wall/TLR2-mediated induction of caspase-dependent programmed cell death. The current study uncovered a third wave of apoptosis occurring prior to entry of bacteria into the cerebrospinal fluid and induced by circulating cell wall or peptidoglycan. Apoptosis of neurons in the dentate gyrus ensued within 12 h of bacteria entering the bloodstream (regardless of route of challenge [Fig. 1 and 2a]) and after 6 h of systemic challenge of mice with cell wall (Fig. 2b). Cortical neurons and astrocytes appeared to be exempt from this injury. Injury was independent of bacteria or leukocytes in the CSF and did not require endothelial binding of bacterial components, since apoptosis persisted in PAFr$^{-/-}$ mice.

Inflammation driven by intravascular cell wall appeared to participate in SAND. Although cell wall is known to induce cellular activation and cytokine production (13, 14), cell wall-challenged animals produced very low amounts of systemic and CSF cytokines at the time of peak SAND. The persistence of SAND in mice treated with anti-TNF antibody further argued against classical cytokine-mediated damage. However, inflammation clearly played a role in SAND since the overexpression of IL-10 strongly attenuated damage. This suggests that an IL-10-regulated, as-yet-undefined damage pathway exists by which inflammation in the peripheral circulation affects apoptosis of CNS neurons. Cell wall has been described to induce blood-brain barrier permeability (41), suggesting a setting in which IL-10 modulation of peripheral inflammatory events could affect the degree of neuronal damage.

Given the multiplicity of pathways invoked by cell wall, optimal therapeutic strategies to improve cerebral function in septic patients would likely require broad anti-inflammatory interventions. Although indomethacin attenuates chronic inflammation due to cranial irradiation (29), dexamethasone was not successful in preventing SAND in the model. In contrast, CDP-choline resulted in significant neuroprotection. CDP-choline provides protection against neuronal death caused by decreased phospholipid biosynthesis following cerebral ischemia (1, 7) and increases phosphatidylcholine formation in neuronal tissues in vitro and in vivo (37). We have previously shown that CDP-choline rescues neurons dying during pneumococcal meningitis by overcoming the partial inhibition by the bacteria of the terminal enzyme in eukaryotic phosphatidylcholine synthesis (56). This study indicates that CDP-choline also protects against SAND. This effect was strong in that neuronal damage was reduced to levels found in uninfected controls. We conclude that SAND arises from a host IL-10-repressible response to intravascular peptidoglycan or cell wall. CDP-choline represents a potential adjunct therapy for pathological effects of cell wall in the context of sepsis.

ACKNOWLEDGMENTS

We are grateful to J. Short, J. Sublett, and R. Rutschman for technical assistance and S. Dixon for photography.

This work was supported by NIAID R01 27913 and the American Lebanese Syrian Associated Charities. Neither funding agency had any role in conducting this work or influencing these results.

The authors declare no competing financial interests.

REFERENCES

1. **Adibhatla, R., and J. Hatcher.** 2002. Citicoline mechanisms and clinical efficacy in cerebral ischemia. J. Neurosci. Res. **70:**133–139.
2. **Bermpohl, B., A. Halle, D. Freyer, E. Dagand, J. Braun, I. Bechman, N. Schroder, and J. Weber.** 2005. Bacterial programmed cell death of cerebral endothelial cells involves dual death pathways. J. Clin. Investig. **115:**1607–1615.
3. **Braun, J., R. Novak, S. Bodmer, J. Cleveland, and E. Tuomanen.** 1999. Neuroprotection by a caspase inhibitor in acute bacterial meningitis. Nat. Med. **5:**298–302.
4. **Braun, J., R. Novak, P. Murray, C. Eischen, S. Susin, G. Kroemer, A. Halle, J. Weber, E. Tuomanen, and J. Cleveland.** 2001. Apoptosis inducing factor mediates microglial and neuronal apoptosis caused by pneumococcus. J. Infect. Dis. **184:**1300–1309.
5. **Braun, J., J. Sublett, D. Freyer, T. Mitchell, J. Cleveland, E. Tuomanen, and J. Weber.** 2002. Pneumococcal pneumolysin and hydrogen peroxide mediate brain cell apoptosis during meningitis. J. Clin. Investig. **109:**19–27.
6. **Burroughs, M., E. Rozdzinski, S. Geelen, and E. Tuomanen.** 1993. A structure-activity relationship for induction of meningeal inflammation by muramyl peptides. J. Clin. Investig. **92:**297–302.
7. **Clark, W., L. Gunion-Rinker, N. Lessov, and K. Hazel.** 1998. Citicoline treatment for experimental intracerebral hemorrhage in mice. Stroke **29:**2136–2140.
8. **Cundell, D., N. Gerard, C. Gerard, I. Idanpaan-Heikkila, and E. Tuomanen.** 1995. *Streptococcus pneumoniae* anchors to activated eukaryotic cells by the receptor for platelet activating factor. Nature **377:**435–438.
9. **Eddleston, M., and L. Mucke.** 1993. Molecular profile of reactive astrocytes—implications for their role in neurologic disease. Neuroscience **54:**15–36.
10. **Erickson, S., F. de Sauvage, K. Kikly, K. Carver-Moore, S. Pitts-Meek, N. Gillett, K. Sheehan, R. Schreiber, D. Goeddel, and M. Moore.** 1994. Decreased sensitivity to tumour-necrosis factor but normal T-cell development in TNF receptor-2-deficient mice. Nature **372:**560–563.
11. **Evans, T.** 2000. Bioassay for tumor necrosis factor-alpha and beta. Mol. Biotechnol. **15:**243–248.
12. **Feldman, C., R. Anderson, R. Cockeran, T. Mitchell, P. Cole, and R. Wilson.** 2002. The effects of pneumolysin and hydrogen peroxide, alone and in combination, on human ciliated epithelium in vitro. Respir. Med. **96:**580–585.
13. **Freyer, D., R. Manz, A. Ziegenhorn, M. Weih, K. Angstwurm, W. Docke, A. Meisel, R. Schumann, G. Schonfelder, U. Dirnagl, and J. Weber.** 1999. Cerebral endothelial cells release TNFa after stimulation with cell walls of *Streptococcus pneumoniae* and regulate iNOS and ICAM-1 expression via autocrine loops. J. Immunol. **163:**4308–4314.
14. **Freyer, D., M. Weih, and J. Weber.** 1996. Pneumococcal cell wall components induce nitric oxide synthase and TNF-alpha in astroglial-enriched cultures. Glia **16:**1–6.
15. **Girardin, S., I. Boneca, J. Viala, M. Chamaillard, A. Labigne, G. Thomas, D. Philpott, and P. Sansonetti.** 2003. Nod2 is a general sensor of peptidoglycan through muramyl dipeptide (MDP) detection. J. Biol. Chem. **278:**8869–8872.
16. **Girardin, S., L. Travassos, M. Herve, D. Blanot, I. Boneca, D. Philpott, P. Sansonetti, and D. Mengin-Lecreulx.** 2003. Peptidoglycan molecular requirements allowing detection by Nod1 and Nod2. J. Biol. Chem. **278:**41702–41708.
17. **Hoffmann, O., N. Keilwerth, M. Bastholm Bille, U. Reuter, K. Angstwurm, R. Schumann, U. Dirnagl, and J. Weber.** 2002. Triptans reduce the inflammatory response in bacterial meningitis. J. Cereb. Blood Flow Metab. **22:**988–996.
18. **Kadoi, Y., S. Saito, F. Kunimoto, T. Imai, and T. Fujita.** 1996. Impairment of brain beta-adrenergic system during experimental endotoxemia. J. Surg. Res. **61:**496–502.
19. **Kim, Y., S. Kennedy, and M. Tauber.** 1995. Toxicity of *Streptococcus pneumoniae* in neurons, astrocytes and microglia in vitro. J. Infect. Dis. **171:**1363–1368.
20. **Koedel, U., A. Bernatowicz, R. Paul, and H. Pfister.** 1995. Experimental pneumococcal meningitis: cerebrovascular alterations, brain edema, and meningeal inflammation are linked to the production of nitric oxide. Ann. Neurol. **37:**313–323.
21. **Laflamme, N., G. Soucy, and S. Rivest.** 2001. Circulating cell wall components derived from gram-negative, not gram positive, bacteria cause a profound induction of the gene-encoding Toll-like receptor 2 in the CNS. J. Neurochem. **79:**648–657.
22. **Lang, R., D. Patel, J. Morris, R. Rutschman, and P. Murray.** 2002. Shaping gene expression in activated and resting primary macrophages by IL-10. J. Immunol. **169:**2253–2263.
23. **Lang, R., R. Rutschman, D. Greaves, and P. Murray.** 2002. Autocrine deactivation of macrophages in transgenic mice constitutively overexpressing IL-10 under control of the human CD68 promoter. J. Immunol. **168:**3402–3411.
24. **Lebel, M. H., B. Freij, G. Syrogiannopoulos, D. Chrane, M. Hoyt, S. Stewart, B. Kennard, K. Olsen, and G. J. McCracken.** 1988. Dexamethasone therapy for bacterial meningitis. N. Engl. J. Med. **15:**964–971.
25. **Leib, S., Y. Kim, L. Chow, R. Sheldon, and M. Tauber.** 1996. Reactive oxygen intermediates contribute to necrotic and apoptotic neuronal injury in an infant rat model of bacterial meningitis due to group B streptococci. J. Clin. Investig. **98:**2632–2639.

26. **Leonard, J., B. Klocke, C. D'Sa, R. Flavell, and K. Roth.** 2002. Strain-dependent neurodevelopmental abnormalities in caspase deficient mice. J. Neuropathol. Exp. Neurol. **61:**673–677.
27. **Majcherczyk, P., H. Langen, D. Heumann, M. Fountoulakis, M. Glauser, and P. Moreillon.** 1999. Digestion of *Streptococcus pneumoniae* cell wall with its major peptidoglycan hydrolase releases branched stem peptides carrying proinflammatory activity. J. Biol. Chem. **274:**12537–12543.
28. **Mitchell, L., H. Smith, J. Braun, K. Herzog, J. Weber, and E. Tuomanen.** 2004. Dual phases of apoptosis in pneumococcal meningitis. J. Infect. Dis. **190:**2039–2046.
29. **Monje, M., H. Toda, and T. Palmer.** 2003. Inflammatory blockade restores adult hippocampal neurogenesis. Science **302:**1760–1765.
30. **Moore, K., R. DeWaal Malefyt, R. Coffman, and A. O'Garra.** 2001. Interleukin-10 and the interleukin-10 receptor. Annu. Rev. Immunol. **19:**683–765.
31. **Nau, R., A. Soto, and W. Bruck.** 1999. Apoptosis of neurons in the dentate gyrus in humans suffering from bacterial meningitis. J. Neuropathol. Exp. Neurol. **58:**265–274.
32. **Odio, C. M., I. Faingezicht, M. Paris, M. Nassar, A. Baltodano, J. Rogers, L. X. Saez, K. D. Olsen, and G. J. McCracken.** 1991. The beneficial effects of early dexamethasone administration in infants and children with bacterial meningitis. N. Engl. J. Med. **324:**1525–1531.
33. **Pauleau, A.-L., and P. J. Murray.** 2003. Role of Nod2 in the response of macrophages to Toll-like receptor agonists. Mol. Cell. Biol. **23:**7531–7539.
34. **Pfeffer, K., T. Matsuyama, T. Kundig, A. Wakeham, K. Kishihara, A. Shahinian, K. Wiegmann, P. Ohashi, M. Kronke, and T. Mak.** 1993. Mice deficient for the 55 kd tumor necrosis factor receptor are resistant to endotoxic shock yet succumb to L. monocytogenes infection. Cell **73:**457–467.
35. **Pfister, H., A. Fontana, M. Tauber, A. Tomasz, and W. Scheld.** 1994. Mechanisms of brain injury in bacterial meningitis: workshop summary. Clin. Infect. Dis. **19:**463–479.
36. **Radin, J., C. Orihuela, G. Murti, C. Guglielmo, P. Murray, and E. Tuomanen.** 2005. β-Arrestin 1 determines the traffic pattern of PAFr-mediated endocytosis of *Streptococcus pneumoniae*. Infect. Immun. **73:**7827–7835.
37. **Rao, A., J. Hatcher, and R. Dempsey.** 2000. Lipid alterations in transient forebrain ischemia: possible new mechanisms of CDP-choline neuroprotection. J. Neurochem. **75:**2528–2535.
38. **Rivest, S., S. Lacroix, L. Vallieres, S. Nadeau, J. Zhang, and N. Laflamme.** 2000. How the blood talks to the brain parenchyma and the paraventricular nucleus of the hypothalamus during systemic inflammatory and infectious stimuli. Proc. Soc. Exp. Biol. Med. **223:**22–38.
39. **Schuchat, A., K. Robinson, J. Wenger, L. Harrison, M. Farley, A. Reingold, L. Lefkowitz, and B. Perkins.** 1997. Bacterial meningitis in the United States. N. Engl. J. Med. **337:**970–976.
40. **Spellerberg, B., D. Cundell, J. Sandros, B. Pearce, I. Idänpään-Heikkilä, C. Rosenow, and H. Masure.** 1996. Pyruvate oxidase as a determinant of virulence in *Streptococcus pneumoniae*. Mol. Microbiol. **19:**803–813.
41. **Spellerberg, B., S. Prasad, C. Cabellos, M. Burroughs, P. Cahill, and E. Tuomanen.** 1995. Penetration of the blood brain barrier: enhancement of drug delivery and imaging by bacterial glycopeptides. J. Exp. Med. **182:**1037–1044.
42. **Sprung, C., P. N. Peduzzi, C. Shatney, R. Schein, M. Wilson, J. Sheagren, and L. Hinshaw.** 1990. Impact of encephalopathy on mortality in the sepsis syndrome. Crit. Care Med. **18:**801–806.
43. **Tauber, M. G., S. L. Kennedy, J. H. Tureen, and D. H. Lowenstein.** 1992. Experimental pneumococcal meningitis causes central nervous system pathology without inducing the 72-kd heat shock protein. Am. J. Pathol. **141:**53–60.
44. **Tettelin, H., K. Nelson, I. Paulsen, et al.** 2001. Complete genome sequence of virulent isolates of *Streptococcus pneumoniae*. Science **293:**498–506.
45. **Tomasz, A.** 1967. Choline in the cell wall of a bacterium: novel type of polymer-linked choline in pneumococcus. Science **157:**694–697.
46. **Tomasz, A., and K. Saukkonen.** 1989. The nature of cell wall-derived inflammatory components of pneumococci. Pediatr. Infect. Dis. J. **8:**902–903.
47. **Tuomanen, E., H. Liu, B. Hengstler, O. Zak, and A. Tomasz.** 1985. The induction of meningeal inflammation by components of the pneumococcal cell wall. J. Infect. Dis. **151:**859–868.
48. **Tuomanen, E. I., A. Tomasz, B. Hengstler, and O. Zak.** 1985. The relative role of bacterial cell wall and capsule in the induction of inflammation in pneumococcal meningitis. J. Infect. Dis. **151:**535–540.
49. **Turrin, N., D. Gayle, S. Ilyin, M. Flynn, W. Langhans, G. Schwartz, and C. Plata-Salaman.** 2001. Pro-inflammatory and anti-inflammatory cytokine mRNA induction in the periphery and brain following intraperitoneal administration of bacterial lipopolysaccharide. Brain Res. Bull. **54:**443–453.
50. **Vallieres, L., and S. Rivest.** 1997. Regulation of the genes encoding IL-6, its receptor, and gp130 in the rat brain in response to Th immune activator lipopolysaccharide and IL-1β. J. Neurochem. **69:**1668–1683.
51. **Wang, H., H. Liao, M. Ochani, M. Justiniani, X. Lin, L. Yang, Y. Al-Abed, H. Wang, C. Metz, E. Miller, K. Tracey, and L. Ulloa.** 2004. Cholinergic agonists inhibit HMGB1 release and improve survival in experimental sepsis. Nat. Med. **10:**1216–1221.
52. **Watson, R., and J. Carcillo.** 2005. Scope and epidemiology of pediatric sepsis. Pediatr. Crit. Care Med. **6:**S3–S5.
53. **Weber, J., P. Moreillon, and E. Tuomanen.** 2003. Innate sensors for Gram positive bacteria. Curr. Opin. Immunol. **15:**408–415.
54. **Yan, J., J. Jung, J. Lee, J. Lee, S. Huh, H. Kim, K. Jung, J. Cho, J. Nam, H. Suh, Y. H. Kim, and D. Song.** 2004. Therapeutic effects of lysophosphatidylcholine in experimental sepsis. Nat. Med. **10:**161–167.
55. **Yoshimura, A., E. Lien, R. Ingalls, E. Tuomanen, R. Dziarski, and D. Golenbock.** 1999. Recognition of gram positive bacterial cell wall components by the innate immune system occurs via toll-like receptor 2. J. Immunol. **63:**1–5.
56. **Zweigner, J., S. Jackwoski, S. Smith, M. van der Merwe, J. Weber, and E. Tuomanen.** 2004. Bacterial inhibition of phosphatidylcholine biosynthesis triggers apoptosis in the brain. J. Exp. Med. **200:**99–106.

Editor: J. N. Weiser